# ABSORPTION CYCLES USING LOW TEMPERATURE HEAT FOR REFRIGERATION AND HEAT PUMPS

**M. Izquierdo[1], M. Venegas[2], M. de Vega[2] and P. Rodríguez[2]**

[1] Instituto de Ciencias de la Construcción Eduardo Torroja (CSIC). C/ Serrano Galvache s/n, 28033 Madrid

[2] Unidad Asociada de Investigación en Energía y Medioambiente del CSIC y la UC3M, Avda. Universidad 30, 28911 Leganés, Madrid

## ABSTRACT

*The use of low temperature heat (between 50 ºC and 90 ºC) is studied to operate absorption machines in two different applications: refrigeration and heat pump cycles. A double stage absorption machine is modelled and simulated. Results are compared for two different absorbent-refrigerant pairs: $H_2O$-$NH_3$ and $LiNO_3$-$NH_3$, in order to determine which one is more adequate for each application. The results obtained show that in the refrigeration cycle the $H_2O$-$NH_3$ solution operates with a COP of 0.29 and the $LiNO_3$-$NH_3$ solution with a COP of 0.32, when it evaporates at –15 ºC, condenses and absorbs refrigerant at 40 ºC and generates vapour at 90 ºC. The results are presented for evaporation temperatures varying between –5 ºC and –40 ºC and condensation temperatures ranging from 15 ºC to 45 ºC. For the absorption machine operating as a heat pump, the $LiNO_3$-$NH_3$ solution reaches a COP of 1.32 and the $H_2O$-$NH_3$ solution a COP of 1.24, when it condenses and absorbs refrigerant at 50 ºC, evaporates at 0 ºC, and generates vapour at 90 ºC. For the heat pump cycle, the results are presented for evaporation temperatures ranging between 0 ºC and 15 ºC. The minimum temperature required in the generators for both cycles, refrigeration and heat pump, are also showed.*

## KEYWORDS

*Low temperature heat, Double stage absorption cycle, Heat pump, Refrigeration, $H_2O$-$NH_3$, $LiNO_3$-$NH_3$*

## 1. INTRODUCTION

In the last years, the interest on refrigeration systems operated with low temperature heat has considerably increased. To take advantage of this heat at low evaporation temperatures, advanced absorption cycles, such as the multistage absorption cycles, should be adopted.

Recent experiences related to the use of low temperature heat using double stage absorption machines include the projects developed by Schweigler *et al.* (1995, 1996, 1998)[1,2,3] and Lamp *et al.* (1998)[4]. Nevertheless, none of these experiments work with temperatures below 0 ºC in the evaporator. Only Erickson (1995)[5] and Mostofizadeh and Butz (1996)[6] describe experiments with lower temperatures using double stage absorption machines. In all the cases only a $H_2O$-$NH_3$ solution is used.

Ziegler and Riesch (1993)[7] theoretically evaluate double stage absorption cycles. They consider two different applications: a refrigeration cycle using a heat source at 100 ºC with an evaporation temperature of –30 ºC and a condensation temperature of 25 ºC, and a heat pump cycle that employs a heat source at 115 ºC with an evaporation temperature of –10 ºC and a condensation temperature of 45 ºC.

Furthermore Thioye (1997a, 1997b)[8,9] developed several studies that predict the behaviour of multistage absorption cycles and, more in detail, those of 4 absorption stages, used in refrigeration.

However, it has not been found any energy analysis of double stage absorption cycles useful to determine the operating conditions of those machines, either working as heat pumps or as refrigerators using different absorbent-refrigerant pairs.

With evaporation temperatures below 0 ºC, the absorbent-refrigerant combination more widely used in absorption machines is the $H_2O$-$NH_3$ solution. However, other pairs such as the $LiNO_3$-$NH_3$, are theoretically and experimentally known. The main advantage of the first over the second is that crystallisation never occurs; on the other hand, the $LiNO_3$-$NH_3$ solution does not require a rectifying column. Thus, the COP of the cycle is improved and, at the same time, the system is simplified.

In the present work, a simulation of a double stage absorption machine is performed to determine its operating conditions working on the refrigeration and on the heat pump cycles, both using a low temperature heat source (below 90 ºC). The simulation is developed using $H_2O$-$NH_3$ and $LiNO_3$-$NH_3$ solutions.

## 2. THERMODYNAMIC PROPERTIES

The thermodynamic properties of the solutions have been obtained using the correlations defined by Pátek and Klomfar (1995)[10], Infante Ferreira (1984)[11],

Mongey *et al.* (1998)[12], as well as by numerical interpolation of the data tabulated in ASHRAE (1993)[13]. Among the available correlations not all of them present the same accuracy and calculation simplicity for the different properties they provide. Depending on these criteria, the following selection has been performed.

For the $LiNO_3$-$NH_3$ solution, the formulations presented by Infante Ferreira (1984)[11] and Aggarwal and Agarwal (1986)[14] give similar results for the vapour-liquid equilibrium relationships. However, Infante Ferreira offers equations for the estimation of more thermodynamic properties. Therefore these equations have been widely used (Wang *et al.*, 1998[15], Thioye, 1997b[9], Altamush Siddiqui, 1994[16], Ayala *et al.*, 1994[17] and Kaushik and Kumar, 1985[18]), thus they will be also used in the present work.

Multiple correlations are available to calculate the properties of the $H_2O$-$NH_3$ solution, beginning with the equations developed by Schulz (1971)[19] and later extended by Ziegler and Trepp (1984)[20] for pressures below 50 bar. More recently, Pátek and Klomfar (1995)[10], Tillner-Roth and Friend (1998)[21], with a formulation based on the Helmholtz free energy, also Mongey *et al*. (1998)[12] and Xu and Goswami (1999)[22] have developed other equations to calculate the thermodynamic properties.

In the present work the equations developed by Pátek and Klomfar are used to determine the vapour-liquid equilibrium properties and the enthalpy of the liquid and gaseous phases. They are preferred due to:

- The accuracy of the results in the working range of the simulated absorption machine. This has been verified by comparison with the data in ASHRAE (1993)[13].
- Their mathematical simplicity.

The specific heat for the liquid and gaseous phases have been calculated by interpolation of the data given in ASHRAE (1993)[13]. The solution specific volume has been computed using the equation proposed by Mongey *et al.* (1998), which is in very good agreement with the data tabulated in ASHRAE.

## 3. MASS AND ENERGY CONSERVATION EQUATIONS

The diagram of the double stage absorption machine used in the simulation is represented in Figure 1 for the $LiNO_3$-$NH_3$ solution and in Figure 2 for the $H_2O$-$NH_3$ solution. A corresponding PTX diagram of the double stage absorption cycle for the $LiNO_3$-$NH_3$ solution is represented in Figure 3.

The operating pressure at the intermediate level corresponds to the pressure maximising the COP of the cycle. The calculated pressure results to be the geometric average of the pressure at the previous and subsequent levels. Thus:

$$P_{MPA} = P_{MPG} = \sqrt{P_e . P_c} \quad (1)$$

The conservation equations of mass and energy used in the model of each component for the double stage machine are detailed below.

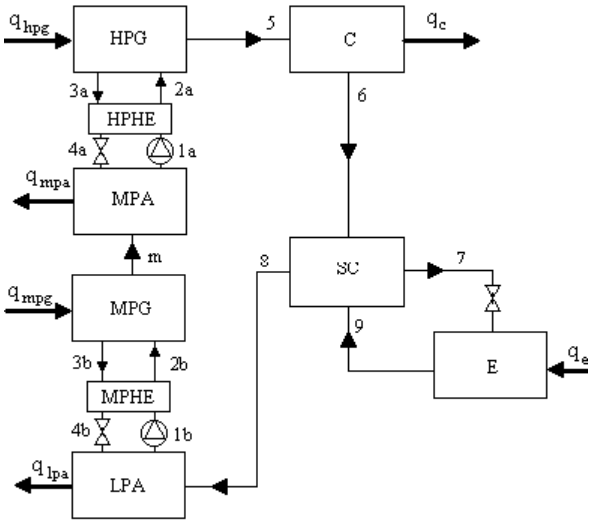


**Figure 1. Double stage absorption machine using the $LiNO_3$-$NH_3$ solution**

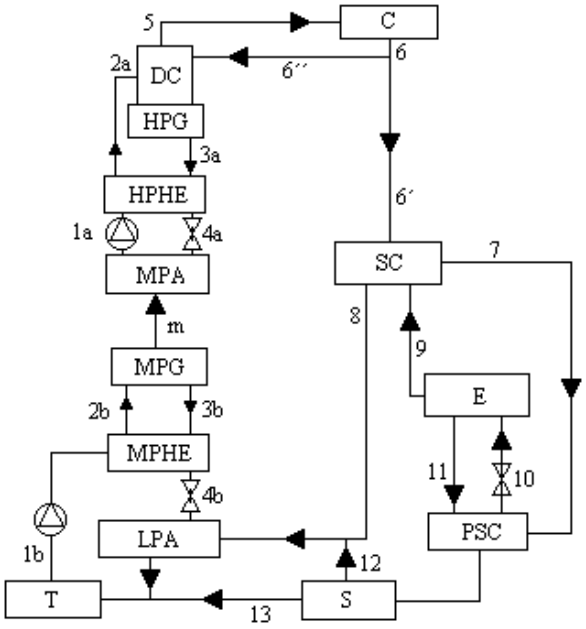


**Figure 2. Double stage absorption machine using the $H_2O$-$NH_3$ solution**

### 3.1 $LiNO_3$-$NH_3$ machine

*Condenser* (C)*:*

$$m_5 = m_6 \quad (2)$$

$$q_c = m_5 h_5 - m_6 h_6 \quad (3)$$

*Sub-cooler* (SC):

$$m_6 = m_7 \tag{4}$$

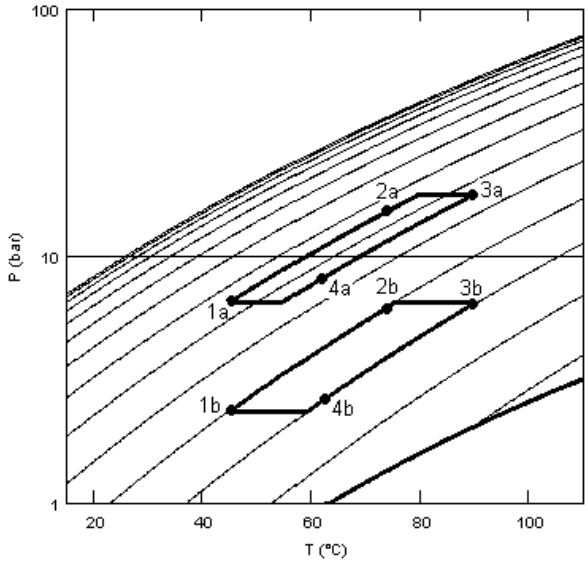


**Figure 3. Thermodynamic cycle of the $LiNO_3$-$NH_3$ double stage absorption machine**

$$m_9 = m_8 \tag{5}$$

$$m_8 h_8 - m_9 h_9 = m_6 h_6 - m_7 h_7 \tag{6}$$

*Evaporator* (E):

$$m_7 = m_9 \tag{7}$$

$$q_e = m_9 h_9 - m_7 h_7 \tag{8}$$

*Middle pressure absorber* (MPA):

$$m_{1a} = m_{4a} + m_m \tag{9}$$

$$q_{mpa} = -m_{1a} h_{1a} + m_{4a} h_{4a} + m_m h_m \tag{10}$$

For the low-pressure absorber (LPA) the points 1a, 4a and *m* are replaced by 1b, 4b and 8 respectively, and $q_{mpa}$ by $q_{lpa}$.

*High pressure heat exchanger* (HPHE):

$$m_{3a} = m_{4a} \tag{11}$$

$$m_{1a} = m_{2a} \tag{12}$$

$$m_{3a} h_{3a} - m_{4a} h_{4a} = m_{2a} h_{2a} - m_{1a} h_{1a} \tag{13}$$

For the middle-pressure heat exchanger (MPHE), 1b, 2b, 3b and 4b replaces the points 1a, 2a, 3a and 4a, respectively.

*Middle pressure generator* (MPG):

$$m_{2b} = m_m + m_{3b} \tag{14}$$

$$q_{mpg} = m_m h_m + m_{3b} h_{3b} - m_{2b} h_{2b} \tag{15}$$

For the high-pressure generator (HPG), the points 2b, 3b and *m* are replaced by points 2a, 3a and 5 respectively, and $q_{mpg}$ by $q_{hpg}$.

The solution flow in the absorbers and generators, per unit of coolant mass separated in the generators, is obtained from a mass balance in each component. For example, for the high-pressure zone:

$$m_{3a} = \frac{x_6 - x_{2a}}{x_{2a} - x_{3a}} \tag{16}$$

In all the cases:

- The heat exchangers efficiency has been considered equal to 70 %.
- The concentrations of the weak and strong solutions correspond to the equilibrium concentrations at the given pressure and temperature.
- The absorption temperature in both absorbers is equal to the condensation temperature.

### 3.2 $H_2O$-$NH_3$ machine

The equations of the condenser, middle-pressure absorber, middle-pressure generator and heat exchangers used in the model of the $H_2O$-$NH_3$ are those described for the $LiNO_3$-$NH_3$.

In the present case ($H_2O$-$NH_3$), the following equation is also to be satisfied because of the presence of the distillation column:

$$m_6 = m_{6'} + m_{6''} \tag{17}$$

where $m_{6'}$ is the coolant mass circulating through the evaporator with a 99.95 % of ammonia (established as a design criterion). $m_{6''}$ is the reflux, calculated for the worst operating conditions.

For the mass and energy balances in the sub-cooler, the equations (4), (5) and (6) are still valid, provided that subscript 6´ replaces the subscript 6 in equation (4) and (6). The mass and energy balances in the remaining components are the following:

*Evaporator* (E):

$$m_{10} = m_9 + m_{11} \tag{18}$$

$$q_e = m_9 h_9 + m_{11} h_{11} - m_{10} h_{10} \tag{19}$$

The evaporator purge parameters are determined according to a 1 % pressure change allowed in the evaporator. With this criterion, we calculate $x_{11}$ using the relationship given by Bogart (1981)[23]:

$$\%\Delta p_e = 0.883\left(1 - x_{11}\right)^{1.042} \tag{20}$$

With this value, $1/K$ is determined for different evaporation temperatures. The composition of the steam that exits the evaporator is calculated according to the relation:

$$1 - x_9 = K(1 - x_{11}) \quad (21)$$

*Low-pressure absorber* (LPA) *(including absorber tank* (T)*):*

$$m_{4b} + m_8 + m_{12} + m_{13} = m_{1b} \quad (22)$$

$$q_{lpa} = m_{4b}h_{4b} + m_8h_8 + m_{12}h_{12} + m_{13}h_{13} - m_{1b}h_{1b} \quad (23)$$

*High-pressure generator* (HPG) *(including distillation column* (DC)*):*

$$m_{2a} + m_{6''} = m_{3a} + m_5 \quad (24)$$

$$q_{hpg} = m_{3a}h_{3a} + m_5h_5 - m_{2a}h_{2a} - m_{6''}h_{6''} \quad (25)$$

The worst operating conditions have been considered to calculate the reflux value. Those occur when the solution that enters the high-pressure generator has the minimum concentration of $NH_3$, which occurs at a condensation and absorption temperatures of 40 ºC.

The calculation of the reflux value has been performed according to the procedure described by Bogart (1981)[23]:

$$m_{6''} = \frac{Ac - h_5}{(h_5 - h_6)\cdot 0.8} \quad (26)$$

where:

$$Ac = \frac{H_2(x_5 - x_2) - h_2(x_5 - y_2)}{y_2 - x_2} \quad (27)$$

The conditions in point 2 correspond to the initial boiling temperature in the high-pressure generator.

*Separator* (S) *and purge sub-cooler* (PSC)*:*

$$m_7 = m_{10} \quad (28)$$

$$m_{11} = m_{12} + m_{13} \quad (29)$$

$$m_{12}h_{12} + m_{13}h_{13} - m_{11}h_{11} = m_7h_7 - m_{10}h_{10} \quad (30)$$

## 4. RESULTS AND DISCUSSION

### 4.1 Refrigeration cycle

In Figure 4 the maximum COP of the double stage cycle at different evaporation temperatures is shown for both solutions, condensing and absorbing refrigerant vapour at 40 ºC with a generation temperature of 90 ºC (temperature of the vapour exiting the generator).

For equal absorption and condensation temperatures ($T_{ac}$), the theoretical temperature relationship for the ideal double stage machine (Annex 24 Final Report)[24] is:

$$T_g^{\,2} \cdot T_e = T_{ac}^3 \quad (31)$$

According to this equation, for a generation temperature of 90 ºC and an absorption and condensation temperature of 40 ºC, a theoretical evaporation temperature of –40 ºC is obtained. For these conditions the ideal COP is 0.4.

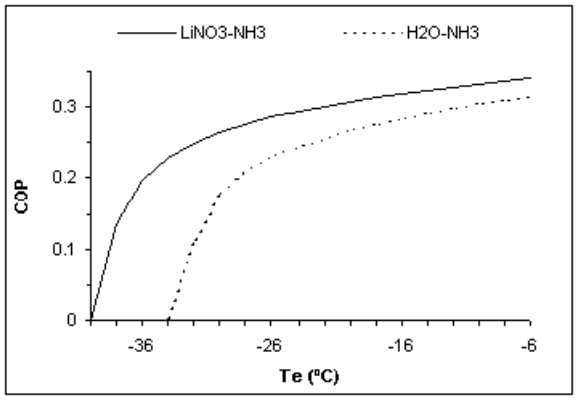


**Figure 4. Maximum COP of the refrigeration cycle**

As it is expected the real evaporation temperatures are higher. For both solutions and an evaporation temperature of –40 ºC the real COP is 0 (Figure 4).

The $LiNO_3$-$NH_3$ solution yields a higher COP for the whole range of evaporation temperatures. It can be seen that the $LiNO_3$-$NH_3$ pair does not work for evaporation temperatures lower than –40 ºC. The $H_2O$-$NH_3$ solution presents a narrower operating range, limited to evaporation temperatures higher than –34 ºC for similar conditions. This limit in the evaporation temperature is due to the fact that the heat supplied to the generators is not enough to separate refrigerant vapour in these conditions.

Furthermore, the $LiNO_3$-$NH_3$ solution requires lower temperatures in the generators to begin its operation than the $H_2O$-$NH_3$ solution (Figure 5), for all the range of evaporation temperatures considered and a condensation and absorption temperatures equal to 40 ºC.

Figure 6 presents the generation temperature needed to operate a double stage refrigeration machine as a function of the condensation temperature, for both solutions and an evaporation temperature equal to –15 °C.

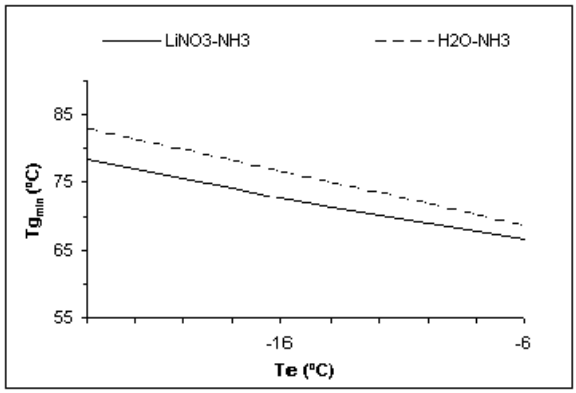


**Figure 5. Minimum generation temperatures in the refrigeration cycle**

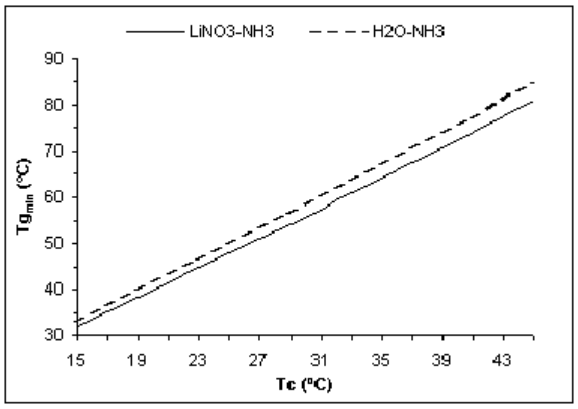


**Figure 6. Minimum generation temperatures to evaporate at –15 ºC**

It can be observed that for the whole range of condensation temperatures the $LiNO_3$-$NH_3$ machine requires a lower generation temperature than the $H_2O$-$NH_3$ system. For lower condensation temperatures both solutions approximate their behaviour. Therefore we can conclude that the $LiNO_3$-$NH_3$ solution would be more advantageous in climatic regions where the ambient temperature is moderately high, as for example the tropical zones.

### 4.2 Heat pump cycle

For the machine operating as a heat pump, the results obtained are shown in Figure 7 and Figure 8. In Figure 7 the maximum COP that would reach the machine at different evaporation temperatures is shown for both solutions, a condensation and absorption temperatures equal to 50 ºC and a generation temperature equal to 90 ºC.

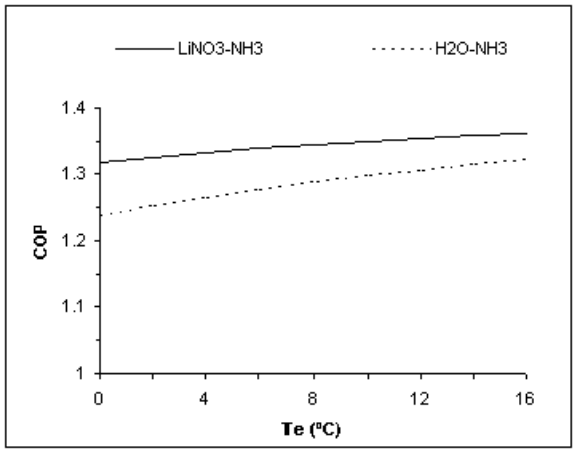


**Figure 7. Maximum COP of the heat pump cycle**

The evaporation temperatures considered extend only to 0 °C because this is the lowest temperature attainable using water as the heat source in the evaporator.

Again, the heat pump cycle using a $LiNO_3$-$NH_3$ solution yields a higher efficiency in the whole range of evaporation temperatures and requires lower temperatures in the generators than the $H_2O$-$NH_3$ solution (Figure 8).

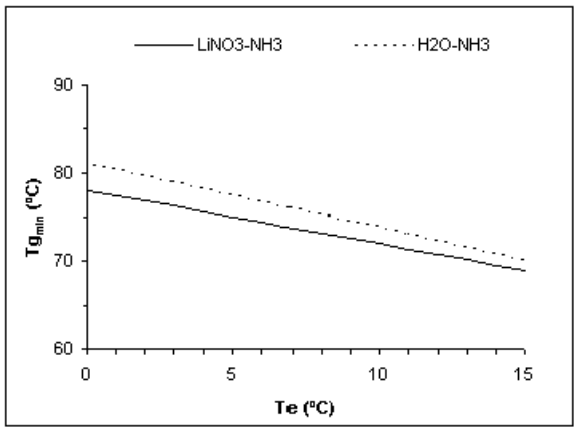


**Figure 8. Minimum generation temperatures in the heat pump cycle**

### 4.3 $LiNO_3$-$NH_3$ crystallisation characteristics

In general the difficulty that the $LiNO_3$-$NH_3$ solution presents is the possibility of crystallisation. In Figure 9, for the refrigeration cycle, the zone between both similar lines represents the valid range of generation temperature without problems of crystallisation, for different condensation temperatures and three evaporation temperatures.

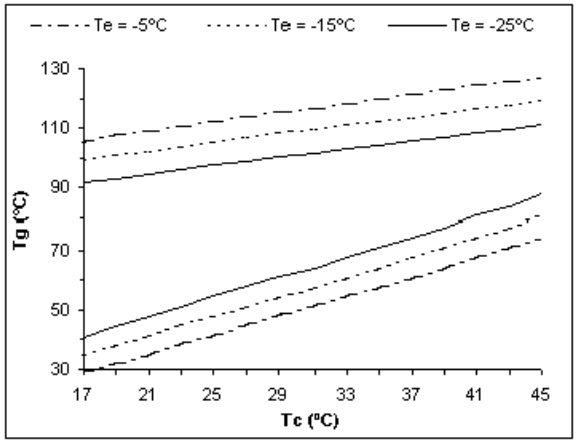


**Figure 9. Working temperatu re range possible in the generators of the $LiNO_3$-$NH_3$ refrigeration cycle**

Figure 9 shows that, low condensation temperatures require low generation temperatures, in accordance to what is expected as the temperature lift is decreased. In a similar way, high evaporation temperatures will require lower generation temperatures.

On the other hand, while the condensation temperature increases and/or the evaporation temperature decreases, the useful range of generation temperatures also decreases, because the temperature

lift is increased. The solution crystallisation line shown in Figure 10 establishes the upper limit to the generation temperature.

Figure 10 shows a typical double stage absorption refrigeration cycle in extreme operating conditions, i.e. evaporation at –25 °C, condensation and absorption at 45 °C and a generation temperature of 90 °C. It can be seen that the operating region is located far away from the crystallisation line.

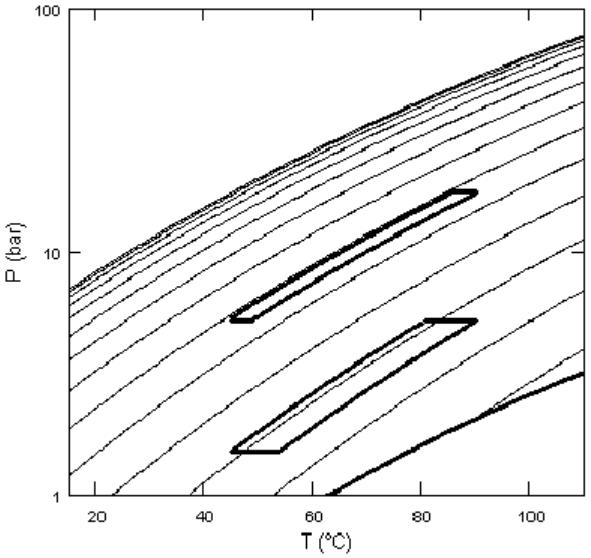


**Figure 10. Typical $LiNO_3$-$NH_3$ double stage absorption refrigeration cycle**

As a final result, in Figure 11 the range of possible working temperatures in the generators for the heat pump is represented, for condensation and absorption temperatures equal to 50 ºC and different evaporation temperatures. It can be appreciated that, while the evaporation temperature decreases, the temperature range also decreases.

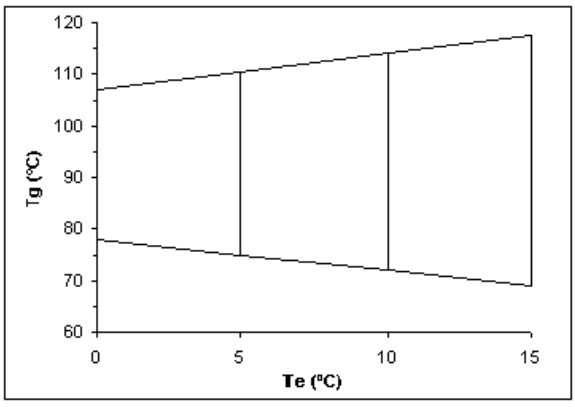


**Figure 11. Working temperature range possible in the generators of the heat pump cycle**

## 5. ECONOMIC ANALYSIS

One prototype of a double stage absorption machine of 5 kW of nominal power will be constructed this year by the Unidad Asociada de Investigación en Energía y Medioambiente del CSIC y la Universidad Carlos III de Madrid.

The estimated cost of the prototype is 34 260 Euros. This cost includes the heat exchange and auxiliary equipment, control and measurement tools, manpower and maintenance. It could foresighted that the unitary costs will decrease when the nominal power increases.

## 6. CONCLUSIONS

The simulation performed permits to conclude:

A- Refrigeration cycle:

1. The double stage refrigeration cycle reaches a higher COP using a $LiNO_3$-$NH_3$ solution than using a $H_2O$-$NH_3$ solution. It can also work with lower evaporation temperatures.
2. In refrigeration cycles the $LiNO_3$-$NH_3$ solution requires lower temperatures to feed the generators than the $H_2O$-$NH_3$ solution. An upper limit exists to the generation temperature settled by the $LiNO_3$-$NH_3$ crystallisation characteristics.
3. To feed the generators of the refrigeration cycle, for moderately high condensation temperatures, the $LiNO_3$-$NH_3$ solution requires substantially lower temperatures than the $H_2O$-$NH_3$ solution. It could be expected to be a good system for tropical zones.

B- Heat pump cycle condensing and absorbing refrigerant vapour at 50 °C:

4. The double stage heat pump absorption cycle reaches a higher COP using a $LiNO_3$-$NH_3$ solution than the one using a $H_2O$-$NH_3$ solution.
5. To feed the heat pump generators, for evaporation temperatures ranging between 0 °C and 15 °C, the $LiNO_3$-$NH_3$ solution requires lower temperatures than the $H_2O$-$NH_3$ solution.

C- Refrigeration and heat pump cycles:

6. The double stage absorption cycles for refrigeration and heat pump purposes are adequate for recovering low temperature heat, below 90 °C.
7. Given the high availability of low temperature residual heat sources and other sources of these characteristics, it is possible to use this heat for refrigeration and heat pump applications using multistage machines. The adequacy of triple stage absorption machines may be studied too, aiming to use even lower temperature heat sources.

## 7. ACKNOWLEGMENTS

The authors wish to express their gratitude to the Ministerio de Ciencia y Tecnología for their interest in the development of absorption refrigeration technology, and the financial support of this research through the Energy Project PROFIT 265 and the Project AMB1999-0211. M. Venegas also wishes to thank to the Agencia Española de Cooperación Internacional for the scholarship granted.

## 8. REFERENCES

[1] C. Schweigler, P. Riesch and G. Alefeld, Using district heating networks for air conditioning, Proc. 19th Int. Congress of Refrigeration, Vol. IIIb, pp 865-872, ISBN 2-903633-79-7 (1995)

[2] C. Schweigler, P. Riesch, S. Demmel and G. Alefeld, A new absorption chiller to establish combined cold, heat, and power generation utilizing low-temperature heat, ASHRAE Transactions, Vol. 102, Pt. 1, pp 1118-1127 (1996)

[3] C. Schweigler, H. Hellman, M. Preissner, S. Demmel and F. Ziegler, Operation and performance of a 350 kW (100 RT) single-effect/double-stage absorption chiller in a district heating network, ASHRAE Transactions, Vol. 104, Pt. 1 (B), pp 1420-1426 (1998)

[4] P. Lamp, C. Schweigler and F. Ziegler, Opportunities for sorption cooling using low grade heat, Applied Thermal Engineering, Vol. 18, pp 755-764, ISSN 1359-4311 (1998)

[5] D.C. Erickson, Waste-heat-powered icemaker for isolated fishing villages, ASHRAE Transactions: Symposia, CH-95-18-3, pp 1185-1188 (1995)

[6] Ch. Mostofizadeh and E. Butz, Use of low-temperature heat to produce deeper temperature refrigeration by means of a new type absorption refrigeration plant, Proc. Int. Ab-sorption Heat Pump Conference, Montreal, Vol. II, pp 633-639, ISBN 0-660-16599-6 (1996)

[7] F. Ziegler and P. Riesch, Absorption cycles. A review with regard to energetic efficiency, Heat Recovery Systems & CHP, Vol. 13, No. 2, pp 147-159, ISSN 0890-4332 (1993)

[8] M. Thioye, Performance improvement of absorption cooling systems by using stage absorption and desorption cycles, Int. J. Refrig., Vol. 20, No. 2, pp 136-145, ISSN 0140-7007 (1997a)

[9] M. Thioye, Performance study of cooling systems using low grade heat energy for refrigeration, Int. J. Refrig., Vol. 20, No. 4, pp 283-294, ISSN 0140-7007 (1997b)

[10] J. Pátek and J. Klomfar, Simple functions for fast calculations of selected thermodynamic properties of the ammonia-water system, Int. J. Refrig., Vol. 18, No. 4, pp 228-234, ISSN 0140-7007 (1995)

[11] C.A. Infante Ferreira, Thermodynamic and physical property data equations for ammonia-lithium nitrate and ammonia-sodium thiocyanate solutions, Solar Energy, Vol. 32, No. 2, pp 231-236, ISSN 0038-092X (1984)

[12] B. Mongey, J.T. McMullan, N.J. Hewitt and G. Molyneaux, An equation of state for $NH_3$-$H_2O$ mixtures, Proc. IIF-IIR - Sections B and E - Oslo, Norway, pp- 443-450 (1998)

[13] ASHRAE, Fundamentals Handbook, SI ed., ISBN 0910110972 (1993)

[14] M.K. Aggarwal and R.S. Agarwal, Thermodynamic properties of lithium nitrate-ammonia mixtures, Energy Research, Vol. 10, pp 59-68, ISSN 0363-907X (1986)

[15] J. Wang, G. Chen and H. Jiang, Study on a solar-driven ejection absorption refrigeration cycle, Int. J. Energy Res., Vol. 22, pp 733-739, ISSN 0363-907X (1998)

[16] M. Altamush Siddiqui, Economic analyses of the operating costs in four absorption cycles for optimizing the generator and condensing temperatures, Energy Convers. Mgmt, Vol. 35, No. 6, pp 517-534, ISSN 0196-8904 (1994)

[17] R. Ayala, J.L. Frias, L. Lam, C.L. Heard and F.A. Holland, Experimental assessment of an ammonia/lithium nitrate absorption cooler operated on low temperature generation, Heat Recovery Systems & CHP, Vol. 14, No. 4, pp 437-446, ISSN 0890-4332 (1994)

[18] S.C. Kaushik and R. Kumar, Thermodynamic study of a two-stage vapour absorption refrigeration system using $NH_3$ refrigerant with liquid/solid absorbents, Energy Convers. Mgmt, Vol. 25, No. 4, pp 427-431, ISSN 0196-8904 (1985)

[19] S.C.G. Schulz, Equations of state for the system ammonia-water for use with computers, Proc. XIIth Int. Congress Refrigeration, Washington. Vol. 2, pp 431-436 (1971)

[20] B. Ziegler and Ch. Trepp, Equation of state for ammonia-water mixtures, Int. J. Refrig., Vol. 7, No. 2, March, pp 101-106, ISSN 0140-7007 (1984)

[21] R. Tillner-Roth and D.G. Friend, A Helmholtz free energy formulation of the thermodynamic properties of the mixture {water + ammonia}, J. Phys. Chem. Ref. Data, Vol. 27, No.1, pp 63-96, ISSN 0047-2689 (1998)

[22] F. Xu and Y. Goswami, Thermodynamic properties of ammonia-water mixtures for power-cycle applications, Energy, Vol. 24, No. 6, pp 525-536, ISSN 0360-5442 (1999)

[23] M. Bogart, Ammonia Absorption Refrigeration in Industrial Processes, Gulf Publishing Company, Texas, ISBN 0-87201-027-9 (1981)

[24] HPC, Annex 24 Final Report, Heat Pump Centre (2000)

## Nomenclature

| | |
|---|---|
| $\%\Delta p_e$ - | pressure loss in the evaporator, % |
| *Ac* - | Ponchon swing-point ordinate at overhead condenser, kJ/kg |
| C - | condenser |
| COP - | coefficient of performance |
| DC - | distillation column |
| E - | evaporator |
| *h* - | liquid specific enthalpy, kJ/kg |
| *H* - | vapour specific enthalpy, kJ/kg |
| HPG, *hpg* - | high pressure generator |
| HPHE - | high pressure heat exchanger |
| *K* - | vapour-liquid equilibrium ratio, y/x |
| LPA, *lpa* - | low pressure absorber |
| *m* - | specific mass flow, kg/kg |
| MPA, *mpa* - | middle pressure absorber |
| MPG, *mpg* - | middle pressure generator |
| MPHE - | middle pressure heat exchanger |
| P- | pressure, bar |
| PSC - | purge sub-cooler |
| *q* - | heat per mass unit, kJ/kg |
| S - | separator |
| SC - | sub-cooler |
| T - | solution tank; temperature, °C |
| *x* - | liquid phase composition, wt % ammonia |
| *y* - | vapour phase composition, wt % ammonia |

*Subscripts*

1a, 1b, 2a, 2b, 3a, 3b, 4a, 4b - points in Figure 2

| | |
|---|---|
| 2 - | conditions at the initial boiling temperature in the HPG |

5, 6, 6´, 6´´, 7, 8, 9, 10, 11, 12, 13 - points in Figure 2

| | |
|---|---|
| c - | condenser |
| e - | evaporator |